RHO-BWI-DP--053

Rockwell Hanford Operations

BWIP SUPPORTING DOCUMENT

RHO-BWI-DP--053

Rev./Chg. No.	Page 1 Of 47
0	Total Pages 47

End Function Activity: Engineered Barriers Department

Project No.: N/A

TI90 003877

CIN No.: N/A Date: N/A

Document Title: Characterization of Reference Umtanum and Cohassett Basalt

Baseline Doc.. Yes ☐ No ☒ Class: N/A

WBS No. or Work Package No.: L2A1

CEI No.: 002

Borehole No.	Stratigraphic Formations:	Doc. Type	Subj. Code
DC-2 DC-4 RRL-2	Umtanum Flow Cohassett Flow	2019	W001

Prepared by (type & sign name): C. C. Allen

Date: 2/85

See reverse side for additional approvals

Abstract

The Basalt Waste Isolation Project (BWIP) Materials Testing Group (MTG) provides large quantities of reference basalt for testing waste package materials under repository conditions, site sorption characteristics and other experimental purposes. This document describes the reference rock materials currently used in testing, namely entablature and colonnade basalt from the Umtanum and Cohassett flows. The data include sampling locations, bulk chemical composition, modal percentages of major phases, and the chemical and mineralogical compositions of these phases.

Data included in this document are contained in MTG controlled notebooks:

RHO-BW-RN-13	Sampling Locations
NB-125	Optical Mineralogy
RN-12, RN-22, RN-23, RDN-147	X-Ray Diffraction
RN-9, N-496	Electron Microprobe
RN-7,16,18,20	Electron Microscope

*	Distribution Name	Mail Address
	RHO-BWIP	
*	V. B. Subrahmanyam	2101M/200E
*	R. G. Johnston	2101M/200E
*	M. B. Strope	2101M/200E
*	C. C. Allen (10)	2101M/200E
*	J. P. McKinley	2101M/200E
*	S. A. Rawson	2101M/200E
*	S. B. Kunkler	2101M/200E
*	K. W. Bledsoe	2101M/200E
*	D. L. Lane	2101M/200E
*	T. E. Jones	2101M/200E
*	R. B. Kasper	2101M/200E
*	G. L. McKeon	2101M/200E
*	H. L. Benny	2101M/200E
*	L. C. Hulstrom	2101M/200E
*	R. A. Carlson	2101M/200E
*	P. F. Salter	MO-407/200E
*	J. R. Burnell	MO-407/200E
*	J. Myers	MO-407/200E
*	D. T. Reed	MO-407/200E
*	M. I. Wood	MO-407/200E
*	R. P. Anantatmula	MO-407/200E
*	R. L. Fish	MO-407/200E
*	P. E. Long	PBB/1100
*	D. G. Horton	PBB/1100
*	K. R. Fairchild	PBB/1100
*	T. O. Early	PBB/1100
*	R. M. Smith	PBB/1100

(Continued on reverse side)

* COMPLETE DOCUMENT (No asterisk, title page/summary of revision page only) —

BASALT

Prepared By: Rockwell (Company & Contract No.) Date: 2/85

Used By: Rockwell (Company)

Release Stamp/Date:

10

OFFICIALLY RELEASED
1985 APR 10 9 31

Acct 3624

DISCLAIMER

Page 2 Of 47	Number SD- BWI-DP-053	Rev./Chg. No. 0

BWIP SUPPORTING DOCUMENT

	Approvals	Date
☒	V. B. Subrahmanyam Author's Manager	2/15/85
☒	V. B. Subrahmanyam Peer Review	2/15/85
☒	R. T. Wilde for Patentability/Sensitive Material	5 March 85
☐	Research/Licensing Manager	
☐	Engineering & Construction Manager	
☒	R. T. Wilde RT Wilde Project Integ./Perf. Assessment Manager	3-27-85
☐	Exploratory Shaft Prog. Manager	
☐	Repository Program Manager	
☐	Associate Director	
☐	Director	
☒	Health, Safety & Environment M. F. Nicol	3/1/85
☒	Quality Assurance P. J. Reder PJ Reder	3/27/85
☒	Configuration Management R. T. Wilde RT Wilde	3-27-85
☒	Project Integration J. Graham, Manager	2/22/85
☒	Licensing M. J. Smith	2/21/85
	End-Function Manager	
☐		
☐		
☐		
☐		
☐		
☐		

Peer Review Identification No(s): 11116

*	Distribution	Name	Mail Address
	PNL		
*	D. G. Coles		3764/216/300
*	J. A. Schramke		Sigma 5/1306/3000
*	S. G. McKinley		3764/215/300
*	M. J. Apted		PSL/424/3000
	WHC		
*	L. E. Thomas		326/22C/300
*	Records Retention		
	Data Package Holders		
*	R. C. Arnett	02	1135J/1100
*	E. B. Ash	23	PBB/1100
*	G. W. Jackson	08	CDC #7
*	H. Babad	01	PBB/1100
*	H. W. Brandt	26	MO-410/600
*	D. J. Brown	04	PBB/1100
*	~~D. J. Carrell~~	~~18~~	~~PBB/1100~~
*	A. E. Cottom	05	PBB/1100
*	H. B. Dietz	09	MO-346/600
*	G. S. Dintsch	20	MO-039/600
*	D. J. Dodds	28	CDC #30
*	R. C. Edwards	29	2101M/200E
*	L. R. Fitch	12	PBB/1100
*	D. L. Oliver	06	1135J/1100
*	R. E. Gephart	13	PBB/1100
*	R. J. Gimera	14	PBB/1100
*	~~K. H. Henry~~	~~16~~	~~PBB/1100~~
*	G. S. Hunt	37	PBB/1100
*	R. E. Johnson	34	PBB/1100
*	~~K. Kim~~	~~38~~	~~CDC #11~~
*	A. D. Krug	39	CDC-1/3000
*	R. K. Ledgerwood	19	PBB/1100
*	J. F. Marron	42	PBB/1100
*	A. J. McElrath	32	RKE/PB
*	~~E. L. Moore~~	~~17~~	~~PBB/1100~~
*	M. F. Nicol	21	PBB/1100
*	S. M. Price	22	PBB/1100
*	M. J. Smith	18	PBB/1100
*	R. L. Snow	41	PBB/1100
*	N. A. Steger	25	MO-040/600
*	A. M. Tallman	16	PBB/1100
*	DOE-RL	10	Fed Bldg/700
*	R. T. Wilde	15	1135J/1100
*	W. F. Todish (orig + 2)	11	1135J/1100
*	BWIP Library	30	PBB/1100

ltr 3/28/85

SD-BWI-DP-053

REV 0

CHARACTERIZATION OF REFERENCE UMTANUM AND COHASSETT BASALT

C. C. Allen
R. G. Johnston
M. B. Strope

Materials Testing Group
Basalt Waste Isolation Project
Rockwell Hanford Operations
Richland, Washington

Introduction

The licensing of a nuclear waste repository in basalt requires a considerable number of experiments to be performed in the presence of host rock to evaluate the waste package materials performance and to determine the radionuclide sorption characteristics of the site. Large quantities of the host rock are required to perform these experiments. Unfortunately, it is very difficult to obtain such large quantities of the host rock from in-situ sources because the proposed repository is at a depth of approximately 1,000 m. In response to this problem, a suitable basalt, reference Umtanum entablature (RUE), was collected from an outcrop and shown to closely match the chemistry of the repository level basalt (Noonan et al., 1981). It is available in the massive amounts (megagram quantities) that are required for waste package testing and other Basalt Waste Isolation Project experimentation. Samples of RUE-1 were collected in the spring of 1980 at Emerson Nipple, located in the SW 1/4 of the NE 1/4 of Section 12, T13N, R23E, elevation 240 m (Figure 1 and Myers et al., 1979, Plate III-3a). Additional samples from the same location, collected in 1982, are designated RUE-2. A nearby reference Umtanum colonnade (RUC) site has also been designated. Samples of RUC-1 were collected in 1980.

Reference sampling sites for Cohassett entablature (RCE) and colonnade (RCC) were established at an exposure in Sentinel Gap, located in the NE 1/4 of the SE 1/4 of Section 10, T15N, R23E, elevation 308 m (Figure 1 and Myers, et al., 1979, Plate III-3b). As of the present report, four sets of reference Cohassett entablature basalt and three sets of reference Cohassett colonnade basalt had been collected.

The reference basalt samples are being used in hydrothermal and sorption experiments to support waste package testing and other investigations by or for the BWIP. The baseline data provided below will facilitate interpretation of the results.

Reference Umtanum Entablature Basalt

The analyses for the Umtanum entablature basalt included optical petrography and point counting, X-ray diffraction (XRD), scanning electron microscopy (SEM), scanning transmission electron microscopy (STEM), energy-

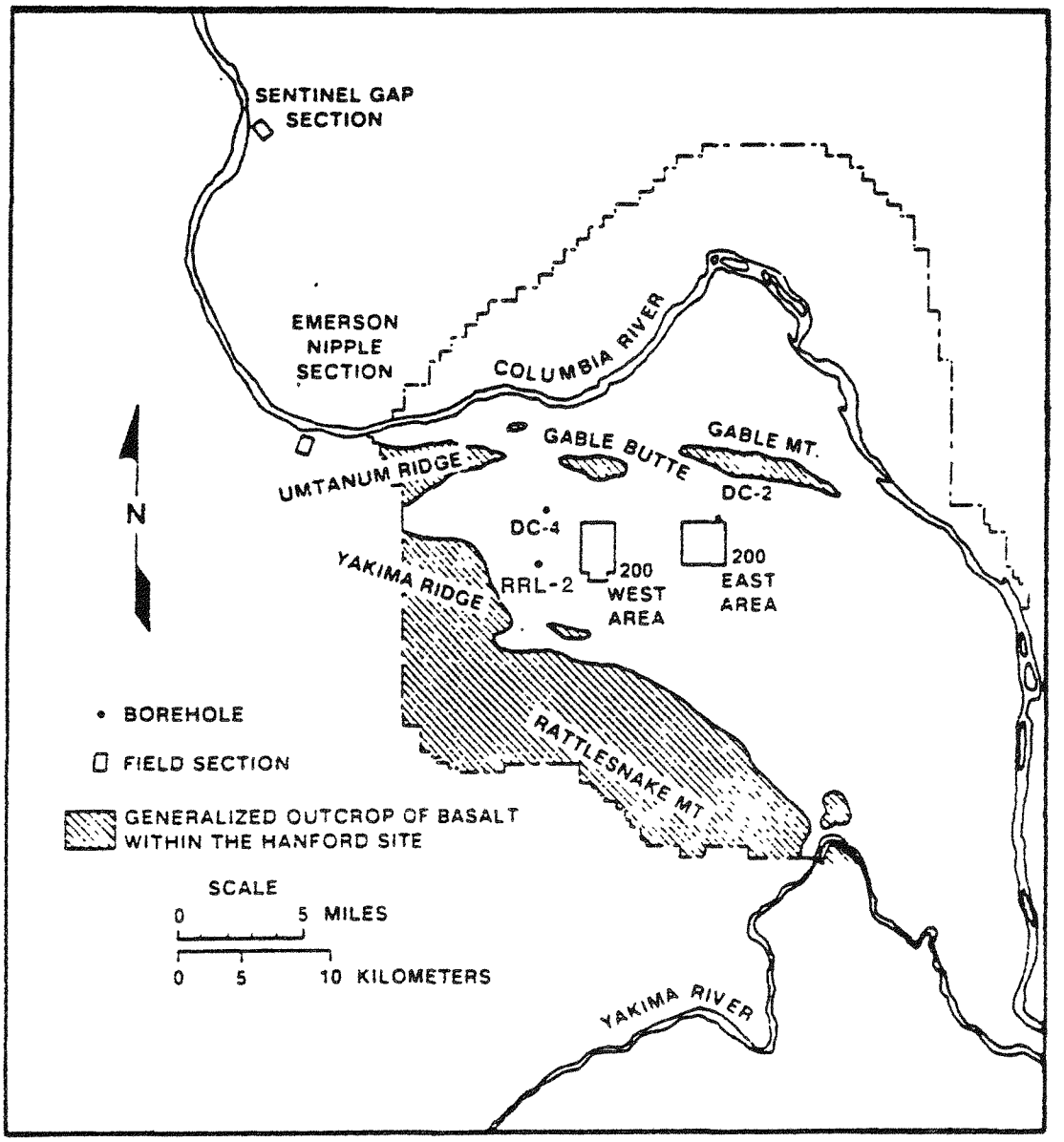

Figure 1. Map of sampling locations (modified from Myers, et al., 1979, Figure III-29).

dispersive spectroscopy (EDS), electron microprobe (EMP), and bulk chemical composition by wet chemistry and X-ray fluorscence (XRF). The petrographic and EMP data are taken from Noonan, et al., (1981) and Palmer, et al., (1982), who measured several thousand points on a number of sections. The wet chemical numbers were obtained on splits from the outcrop.

Petrographic and Microprobe Analysis

The reference Umtanum entablature (RUE) is characterized by abundant glassy mesostasis and titaniferous magnetite dendrites (Figure 2). Plagioclase is the most abundant silicate mineral (Tables 1, 2) and is very constant in composition (An_{49-51}). Clinopyroxene is the second most abundant phase and shows the chemical varieties normally found in basaltic rocks. Most pyroxene is in the augite compositional range with the exception of minor pigeonite, subcalcic augite, and ferroaugite. The major opaque phase is titaniferous magnetite which is nearly constant in composition ranging from 28 - 32 wt.% TiO_2 (Noonan et al., 1981, p. 53). By far the most abundant material in the basalt is the mesostasis (Table 3). This is a Si-rich glass containing micron-size magnetite, pyroxene and apatite crystals (Allen and Strope, 1983, p. 2).

X-ray Diffraction

X-ray diffractograms of the Umtanum entablature basalt from a core sample (DC-4, 3,730.5) and from a surface sample (RUE-2) are compared in Figure 3. The most abundant phase in the basalt is plagioclase feldspar, as indicated by the relative intensities of its major diffraction peaks. The plagioclase diffraction pattern provides good matches with two Powder Diffraction File (PDF) patterns (18-1202: $An_{67.2}$, $Ab_{31.5}$, $Or_{1.35}$; 9-465: $An_{64.5}$, $Ab_{37.2}$, $Or_{2.8}$), listed as intermediate and low sodian anorthite, respectively. Small differences in the peak positions relative to the reference diffractograms are consistent with the composition of the plagioclase (more sodic and potassic than the reference materials) as determined by electron microprobe. The remainder of the peaks may be accounted for by the pyroxene phases augite (PDF 24-201, $Ca[Fe,Mg]Si_2O_6$, and 24-202, $Ca[Mg,Al,Fe]Si_2O_6$) and pigeonite (PDF 13-421, $Fe_{0.48}Mg_{0.45}Ca_{0.04}SiO_3$). Due to the relatively small quantity present and overlaps with the major diffraction peaks of the pyroxenes, the presence of titaniferous magnetite

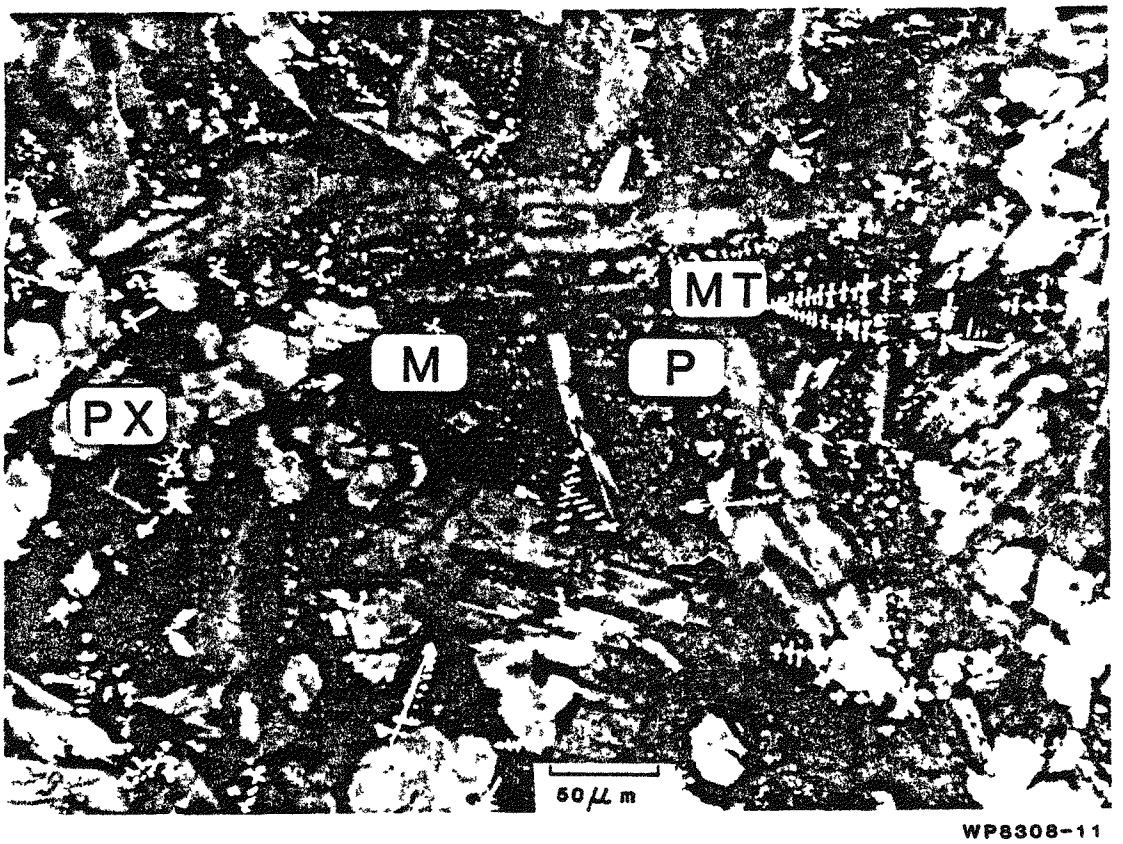

Figure 2. Reflected light photomicrograph of RUE-1 basalt. Plagioclase (P), pyroxene (PX), mesostasis (M), magnetite (MT).

Table 1. Point Count Data* for RUE-1.

Run No.	1	2	3	4	Total	σ
Number of points per run	614	571	671	713	2,569	
Phase	modal %	modal %	modal %	modal %	modal %	+/-
Plagioclase	29.3	27.3	27.9	30.3	28.7	1.4
Pyroxene	16.4	18.6	17.9	15.4	17.1	1.4
Mesostasis	47.1	48.0	47.5	48.1	47.7	1.1
Titaniferous Magnetite	4.72	4.90	5.96	4.91	5.12	0.50
Alteration Products	2.40	1.58	1.34	1.26	1.65	0.52
Total	99. 9	100.4	100.6	100.0	100.3	

* Data from Palmer, et al., 1982, Table 2.

σ = Standard Deviation

TABLE 2. Composition of Major Silicate Minerals* in the Umtanum Entablature (wt %)

	Plagioclase		Pigeonite		Augite	
Oxide	RUE-1	DC-2, 3131	RUE-1	DC-2, 3131	RUE-1	DC-2, 3131
SiO_2	55.5	56.1	50.9	51.5	49.4	50.1
TiO_2	0.11	0.13	0.58	0.61	1.15	0.94
Al_2O_3	27.2	26.6	0.82	0.72	1.89	2.03
FeO[a]	0.70	0.90	23.5	22.5	17.9	15.3
MnO	ND[b]	ND	0.53	0.48	0.46	0.48
MgO	0.11	0.08	19.1	18.1	13.9	14.8
CaO	9.67	9.76	5.2	6.27	15.2	15.1
Na_2O	4.97	5.09	0.07	0.09	0.25	0.28
K_2O	0.68	0.71	ND	ND	ND	ND
P_2O_5	ND	ND	ND	ND	ND	ND
Cr_2O_3	ND	ND	<0.05	<0.05	<0.05	<0.05
TOTAL	98.9	99.4	100.7	100.3	100.2	99.0
Mol%	An 51	An 51	En 53	En 51	En 40	En 43
	Ab 44	Ab 45	Fs 37	Fs 36	Fs 29	Fs 25
	Or 5	Or 4	Wo 10	Wo 13	Wo 31	Wo 32

*Microprobe data from Noonan et al., 1981, Table 2

[a] All iron reported as FeO

[b] ND = not detected

Table 3. Composition of Mesostasis* in the Umtanum Entablature (wt.%)[a]

Oxide	RUE-1	DC-2, 3131
SiO_2	61.2	69.4
TiO_2	1.53	0.86
Al_2O_3	12.5	13.7
FeO[b]	10.5	4.49
MnO	0.16	<0.05
MgO	0.59	<0.05
CaO	3.87	1.90
Na_2O	7.1	7.5
K_2O	2.68	2.74
P_2O_5	0.62	0.36
Cr_2O_3	ND[c]	ND
Total	100.8	101.0

* Microprobe data from Noonan, et al., 1981, Table 3.

[a] Average of five analyses (RUE-1); seven analyses (DC-2, 3131)

[b] All iron reported as FeO

[c] ND = Not detected.

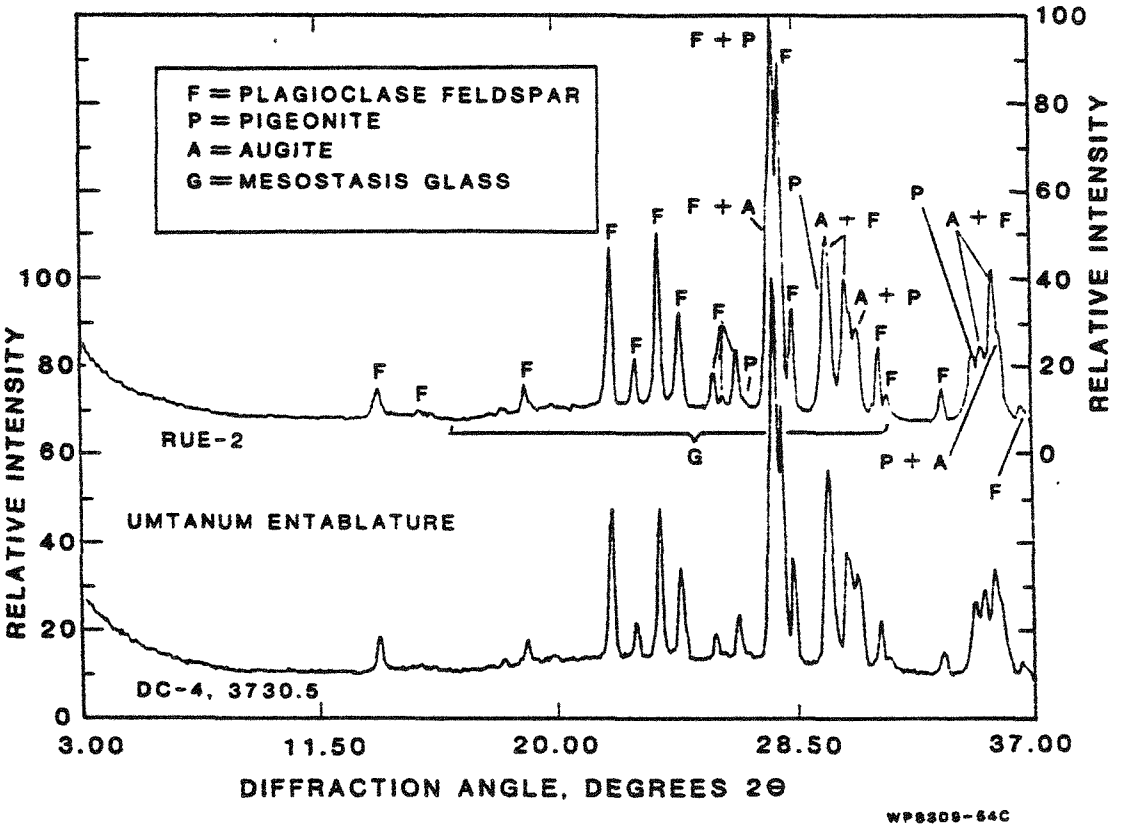

Figure 3. X-ray diffractograms of Umtanum entablature basalt from a surface sample (RUE-2) and a core sample (DC-4, 3730.5). All diffractograms were produced from randomly-oriented powder mounts, using copper Kα radiation.

could not be confirmed by XRD. The weak, very broad humps seen in the background of the diffractograms are a product of the mesostasis glass. No evidence of alteration products (clays) was observed in these diffractograms. Petrographic data indicate that these phases are present in quantities too small for detection by bulk XRD.

The major difference between the Umtanum entablature core and surface samples which is apparent in the diffractograms is in the relative abundance of the pyroxenes (see Figure 3). The core sample contains a larger amount of pigeonite relative to augite than does the surface sample. This variation is consistent with observations by Allen and Strope (1983, p. 2), indicating that pigeonite abundance varies significantly in entablature samples. The diffractograms of the two surface samples, RUE-1 and RUE-2, are nearly identical except for the peak at 3.5^{o} 2θ (Figure 4). This peak is possibly produced by a clay, although no other clay lines are apparent in the pattern.

X-ray Flourescence Data

Several size fractions of material are used in repository experiments. There has been some question as to whether or not the processing of the bulk material by grinding and sieving has selectively fractionated some of the basalt minerals. To demonstrate that this type of artifact was not being produced, XRF analyses of the largest fraction (-16 + 60 mesh) were compared with that of the fraction usually involved in testing (-120 + 230 mesh). These results are presented in Table 4 and show that no significant bias is introduced. These data compare closely to XRF analyses of bulk samples from the RUE surface exposure and core (Table 5).

Surface Area

Salter et al. (1981) used the ethylene glycol absorption method to determine the surface area of a sample of Umtanum basalt sized from 0.30 to 0.85 mm. The value reported was 17.7 ± 3.8 m^2/g.

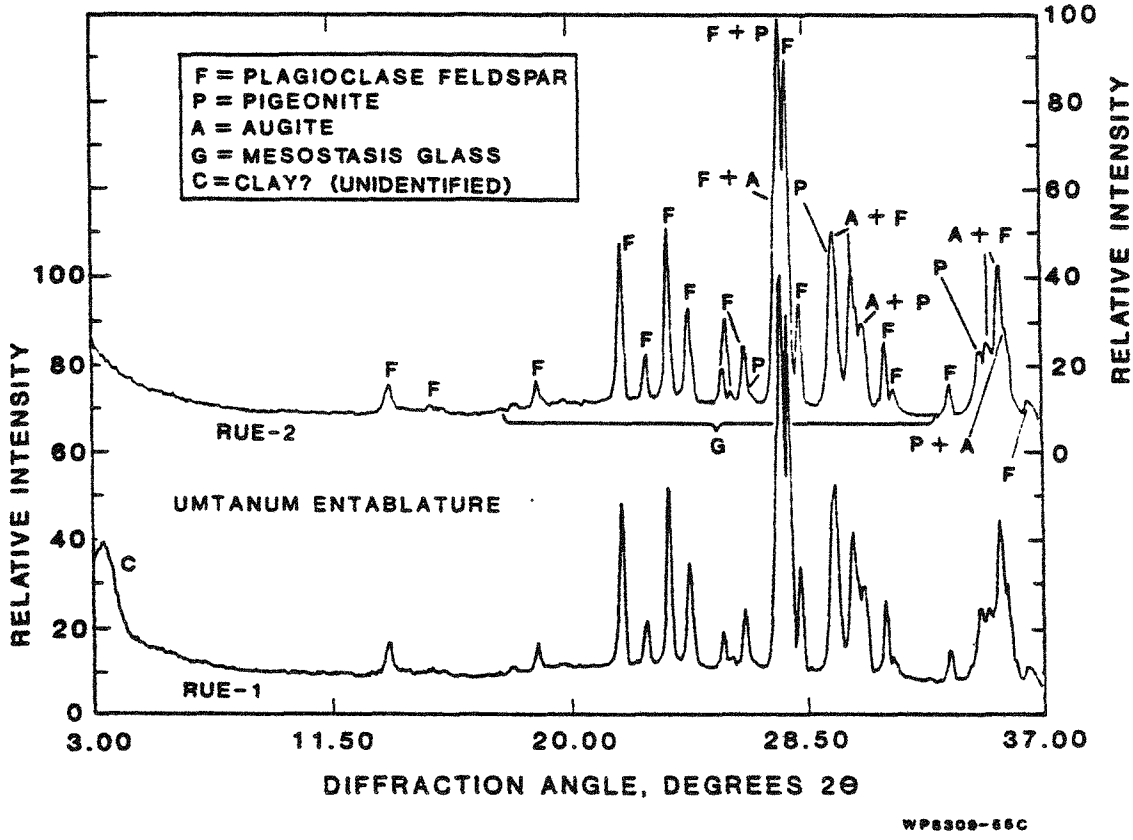

Figure 4. X-ray diffractograms of Umtanum entablature basalt from surface samples RUE-1 and RUE-2, both in -120 +230 mesh size fractions. The clay peak (C) observed in the RUE-1 specimen is consistent with the alteration products phase reported in point count results from other RUE-1 samples (Table 1).

Table 4. Normalized Bulk Analysis* of RUE-1 By XRF (wt%).

	RUE-1 -120 + 230 Mesh	RUE-1 -16 + 60 mesh
SiO_2	54.54	54.93
TiO_2	2.17	2.20
Al_2O_3	15.20	14.78
Fe_2O_3**	2.00	2.00
FeO	10.64	10.94
MnO	0.24	0.21
MgO	3.75	3.50
CaO	7.07	6.98
Na_2O	2.45	2.50
K_2O	1.59	1.61
P_2O_5	0.35	0.35
Total	100.00	100.00

* Data from Palmer, et al., 1982, Table 4.

** Fe_2O_3 arbitrarily set equal to 2.00.

Table 5. Normalized Bulk Analyses by XRF of Umtanum Basalt from Surface Exposures and Core (wt%)

	Surface entablature and colonnade[a]	Core entablature[b]	Core colonnade[c]
SiO_2	54.60	54.88	54.73
TiO_2	2.17	2.13	2.17
Al_2O_3	14.77	14.28	14.65
Fe_2O_3[d]	2.00	2.00	2.00
FeO	10.79	11.08	10.86
MnO	0.22	0.22	0.22
MgO	3.42	3.44	3.39
CaO	7.21	7.30	7.23
Na_2O	2.67	2.70	2.77
K_2O	1.81	1.62	1.62
P_2O_5	0.36	0.35	0.36
Total	100.02	100.00	100.00

[a]Myers et al. (1979), Plate III-3a.

[b]DC-2, 3044.

[c]DC-4, 3741.3.

[d]Fe_2O_3 arbitrarily set equal to 2.00.

Summary

The RUE basalt consists of glassy mesostasis, plagioclase, pyroxene, titaniferous magnetite, and minor clay. Comparisons of surface and core samples indicate that the RUE material should serve in geochemical studies as an adequate substitute for material from the proposed repository depth.

Reference Umtanum Colonnade Basalt

Anaysis of reference Umtanum colonnade (RUC) samples employed some of the techniques listed above. A single sampling trip yielded reference sample RUC-1 (Noonan et al., 1981, p. 52). In addition, earlier sampling of the same horizon near the reference site yielded samples C 8098, C 8099 and C 8100 (Myers et al., 1979, Plate III-3a).

Petrographic and Microprobe Analysis

Basalt from the RUC horizon contains the same major minerals as the RUE basalt (Tables 6 and 7). The colonnade samples are more coarsely crystalline and contain significantly more plagioclase and less mesostasis than does RUE-1. Comparison of Table 7 with Table 2 indicates that the colonnade and entablature plagioclase compositions are essentially identical. These tables also show that the colonnade augite contains more MgO, and the pigeonite less MgO, than do the respective entablature crystals.

The average composition of RUC-1 mesostasis is listed in Table 8. Comparison with the RUE-1 mesostasis (see Table 3) indicates that the mesostasis in the Umtanum colonnade is more "evolved" (i.e., silicon-rich) than that in the entablature, and is similar to that seen in the Cohassett colonnade samples (below).

X-ray Diffraction

Characterization of the Umtanum colonnade basalt by X-ray diffraction has been relatively limited. Analyses of different size fractions of crushed and blended basalt from the surface sample (RUC-1) produce diffractograms

Table 6. Point Count Data* (modal %) for the Reference Umtanum Colonnade Horizon (Samples C 8098, C 8099, C 8100).

	C 8098	C 8099	C 8100
Plagioclase	34.8	38.0	35.9
Pyroxene	19.2	16.5	18.6
Mesostasis	38.2	38.5	37.9
Titaniferous magnetite	5.23	4.75	4.88
Apatite	0.95	1.00	0.98
Alteration products	0.48	0.03	0.43
Total	98.9	98.8	98.7
Points Counted	4,000	4,000	4,000

* Analyses by K. R. Fairchild

Table 7. Composition of Major Silicate Minerals* in the Umtanum Colonnade (wt%).

Oxide	Plagioclase		Pigeonite		Augite	
	RUC-1	DC-2, 3159	RUC-1	DC-2, 3159	RUC-1	DC-2, 3159
SiO_2	56.3	57.3	50.8	51.4	50.1	49.8
TiO_2	0.11	0.09	0.57	0.52	1.05	0.94
Al_2O_3	27.0	26.6	0.90	0.80	2.53	1.71
FeO[a]	0.79	0.84	24.5	21.7	15.6	16.1
MnO	ND[b]	ND	0.67	0.50	0.36	0.39
MgO	0.09	0.06	17.8	20.4	15.5	14.8
CaO	9.4	9.4	5.91	4.81	15.3	15.0
Na_2O	5.3	5.1	0.07	0.09	0.27	0.23
K_2O	0.69	0.78	ND	ND	ND	ND
P_2O_5	ND	ND	ND	ND	ND	ND
Cr_2O_3	ND	ND	<0.05	<0.05	<0.05	<0.05
Total	99.7	100.2	101.2	100.2	100.7	99.0
mol%	An49 Ab47 Or4	An50 Ab45 Or5	En50 Fs38 Wo12	En57 Fs34 Wo 9	En44 Fs25 Wo31	En43 Fs26 Wo31

* Microprobe data from Noonan, et al., 1981, Table 1.

[a]All iron reported as FeO.

[b]ND = Not detected.

Table 8. Composition of Mesostasis* in the Umtanum Colonnade (wt%).[a]

Oxide	RUC-1	DC-2, 3159
SiO_2	72.2	72.9
TiO_2	0.69	0.88
Al_2O_3	12.5	12.7
FeO[b]	1.59	2.16
MnO	<0.05	<0.05
MgO	<0.05	ND[c]
CaO	0.51	0.62
Na_2O	4.01	6.6
K_2O	6.5	4.07
P_2O_5	0.12	0.10
Cr_2O_3	ND	ND
Total	98.1	100.0

* Microprobe data from Noonan et al., 1981, Table 3.

[a]Average of seven analyses.

[b]All iron reported as FeO

[c]ND = Not Detected.

which are very similar to patterns which characterize samples of the Umtanum entablature (Figure 5). The plagioclase patterns are nearly identical, and support microprobe evidence of the essentially identical plagioclase chemistries in both colonnade and entablature. The pyroxene diffraction lines are less similar, with the pigeonite pattern more clearly resolved in the colonnade. The pyroxenes appear to be similar to those present in the entablature, yielding diffraction patterns which also match the reference diffractograms. As in the entablature, no X-ray diffraction evidence of alteration products (clay) was observed, and the presence of titaniferous magnetite could not be confirmed. The broad background hump indicative of mesostasis glass is less intense in the colonnade diffractogram than in that of the entablature, suggesting that a smaller amount of noncrystalline material is present.

The diffractogram of the Umtanum colonnade core specimen differs somewhat from surface colonnade material (Figure 6). The core sample diffractogram suggests that small amounts of potassium feldspar and cristobalite may be present in the specimen. Differences in the relative abundances of augite and pigeonite, and possibly in the composition of the pigeonite (see Table 7) are implied by intensity and shape changes of the pyroxene peaks. The pyroxene peaks are particularly well resolved in this sample, especially at higher diffraction angles.

X-ray Fluorescence

The bulk chemical composition of Umtanum colonnade basalt, as determined by XRF, is given in Table 5. No significant differences exist between the bulk compositions of colonnade and entablature samples, nor between samples collected at the surface and from deep drill cores.

Summary

The reference Umtanum colonnade basalt, based on limited characterization, resembles the reference Umtanum entablature material in terms of bulk chemical composition and mineralogy. However, the major minerals and, to a greater extent, the mesostasis differ significantly in chemical composition.

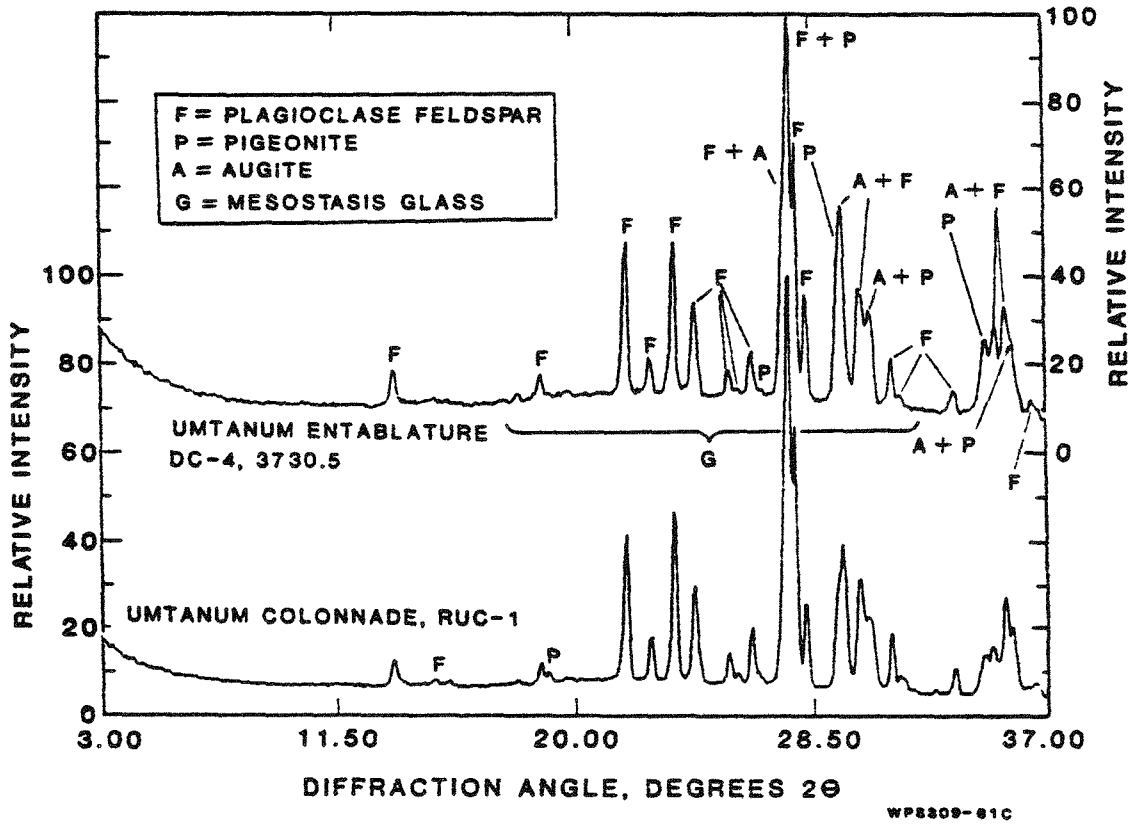

Figure 5. Comparison of X-ray diffractograms from the Umtanum entablature and colonnade.

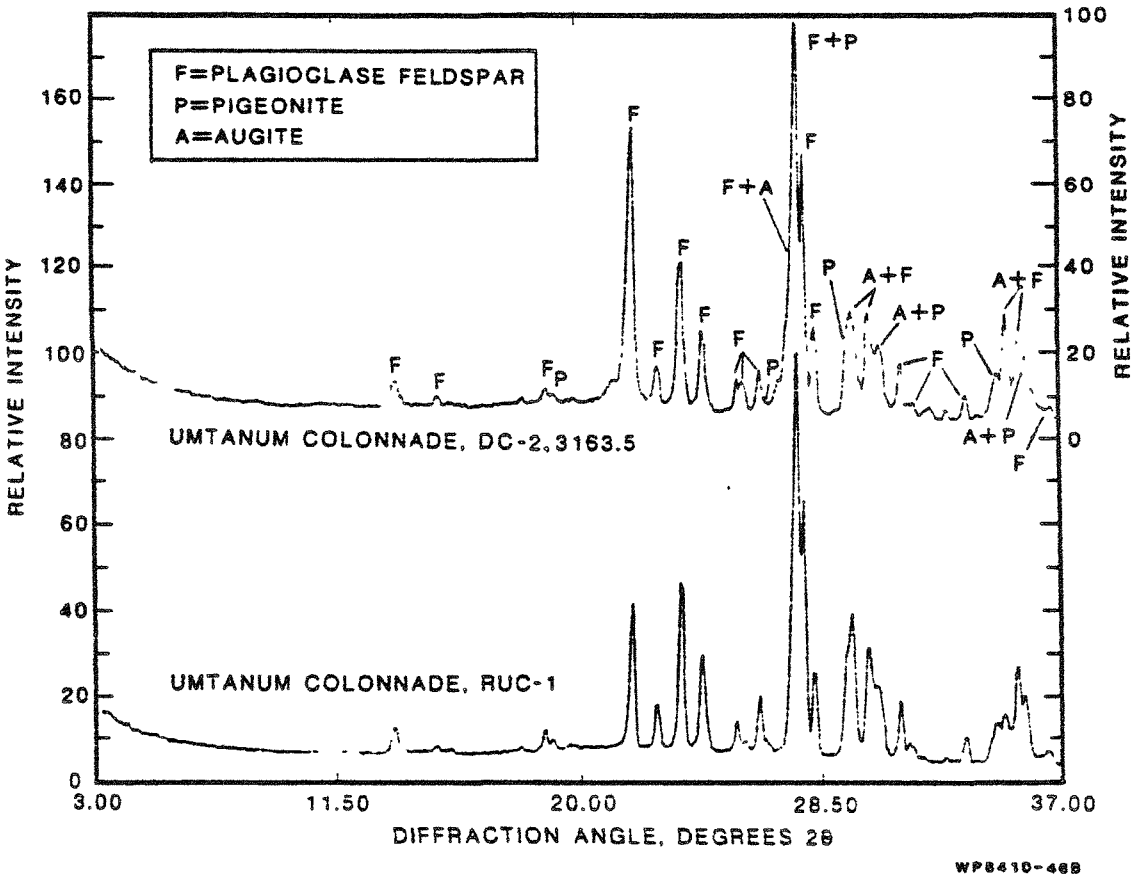

Figure 6. X-ray diffractograms of core (DC-2, 3163.5) and surface (RUC-1) samples of Umtanum colonnade.

Reference surface samples are very similar to core samples from the same horizon.

Reference Cohassett Entablature Basalt

Analysis of reference Cohassett entablature (RCE) samples employed the suite of techniques listed above. As of this report, four sampling trips had produced reference material designated RCE-1, RCE-2, RCE-3 and RCE-4. In addition, previous sampling of the same horizon in the near vicinity of the reference site yielded samples C 9015 and C 9016 (Myers et al., 1979, Plate III-3b).

Petrographic and Microprobe Analysis

The RCE basalt is grossly similar to the Umtanum entablature material described above. The dominant phases are plagioclase, augite, pigeonite, dendritic titaniferous magnetite, and mesostasis (Tables 9, 10). The mean dimensions of the plagioclase and pyroxene crystals, however, are characteristically 2 to 5 times larger in Cohassett basalt than in Umtanum samples. In addition, Cohassett samples contain significantly larger volumes of alteration products, mainly clay, than do Umtanum samples. The texture of a typical section of RCE-1 is shown in Figure 7.

Mesostasis, as defined by point counting, comprises approximately 30 modal % of the basalt from the RCE horizon (see Table 9). Over half of this amount is optically amorphous silica-rich glass (Table 11). The remainder, (Figure 8) consists of micron-scale plagioclase crystals and microcrystalline blebs containing pyroxene, magnetite, and apatite (Allen and Strope, 1983, p.2).

X-ray Diffraction

X-ray diffractograms of Cohassett entablature basalt from a core sample (RRL-2, 3134) and from a surface sample (RCE-1) are compared in Figure 9. Plagioclase feldspar is the most abundant phase in the basalt, as indicated by the relative intensities of its major diffraction peaks. The plagioclase

Table 9. Point Count Data* (modal %) for the Reference Cohassett Entablature Horizon (Samples C 9015, C 9016).

	C 9015	C 9016
Plagioclase	36.5	37.3
Pyroxene	20.6	21.0
Mesostasis	30.5	32.5
Titaniferous magnetite	3.70	4.60
Apatite	TRACE	TRACE
Alteration products	8.30	5.03
Total	99.6	100.4
Points counted	4,000	4,000

* Analyses by K. R. Fairchild

Table 10. Composition of Major Silicate Minerals (wt%) from the Reference Cohassett Entablature Horizon (Sample C 9016).

	Plagioclase		Pigeonite		Augite	
	$\bar{x}$	σ	$\bar{x}$	σ	$\bar{x}$	σ
SiO_2	53.2	0.9	52.9	0.5	52.0	0.6
TiO_2	---	---	0.4	0.1	0.7	0.1
Al_2O_3	28.5	0.6	0.7	0.2	1.7	0.5
FeO*	0.8	0.1	19.9	0.9	11.5	2.0
MnO	---	---	0.5	0.0	0.3	0.0
MgO	0.2	0.1	20.4	1.0	16.0	0.8
CaO	11.8	0.8	4.9	0.9	17.1	1.4
Na_2O	4.6	0.5	0.1	0.1	0.2	0.1
K_2O	0.3	0.1	0.0	0.0	0.0	0.0
P_2O_5	---	---	---		---	
Total	99.4		99.8		99.5	
Points analyzed by microprobe = 55			9		18	
mol%	An 58 Ab 41 Or 2		En 58 Fs 32 Wo 10		En 46 Fs 19 Wo 35	

$\bar{x}$ Mean

σ Standard Devation

* All iron reported as FeO

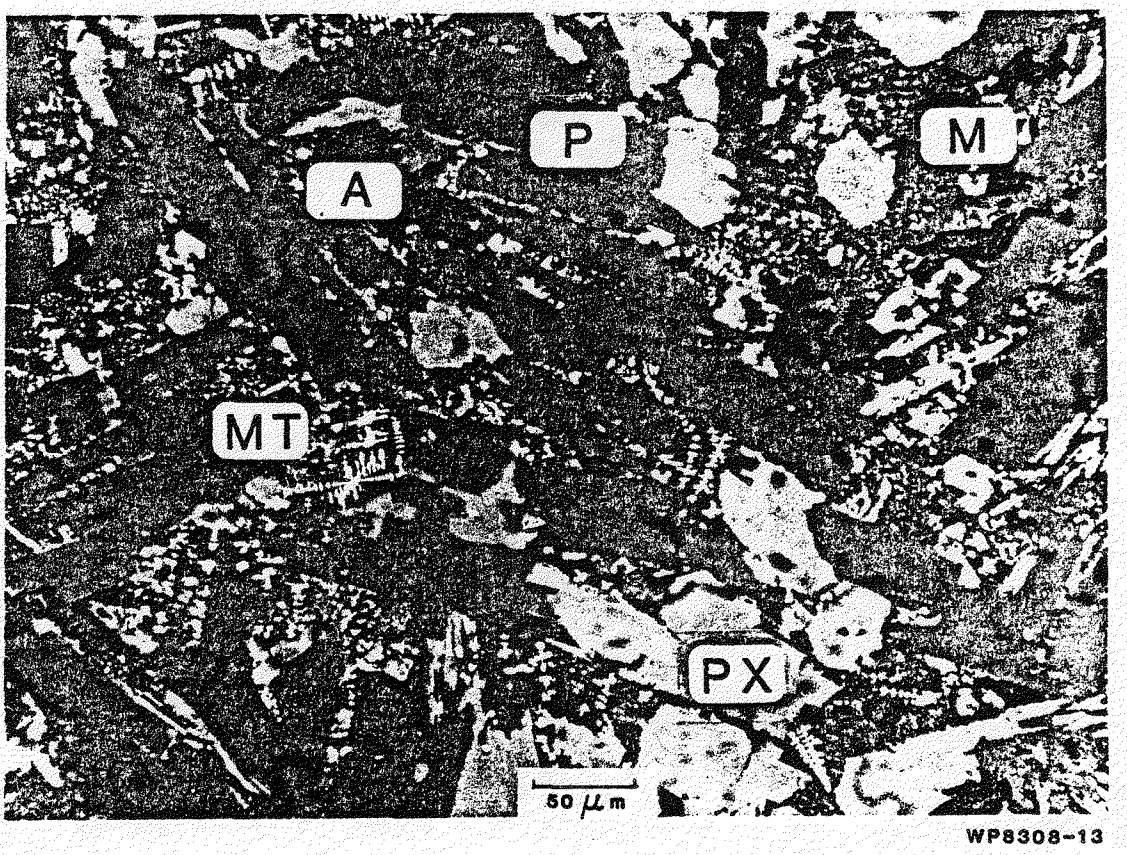

Figure 7. Reflected light photomicrograph of RCE-1 basalt. Plagioclase (P), pyroxene (PX), mesostasis (M), magnetite (MT), alteration (A).

Table 11. Composition of Mesostasis Glass (wt%) from the Reference Cohassett Entablature Horizon (Sample C 9016)

	$\bar{x}$	σ
SiO_2	65.1	3.2
TiO_2	1.0	0.6
Al_2O_3	14.0	2.1
FeO*	5.4	2.4
MnO	0.4	0.1
MgO	0.5	0.8
CaO	3.1	1.4
Na_2O	4.2	0.9
K_2O	3.4	1.0
P_2O_5	0.6	0.2
Total	97.7	

Points analyzed by microprobe = 68

$\bar{x}$ Mean

σ Standard Deviation

* All iron reported as FeO

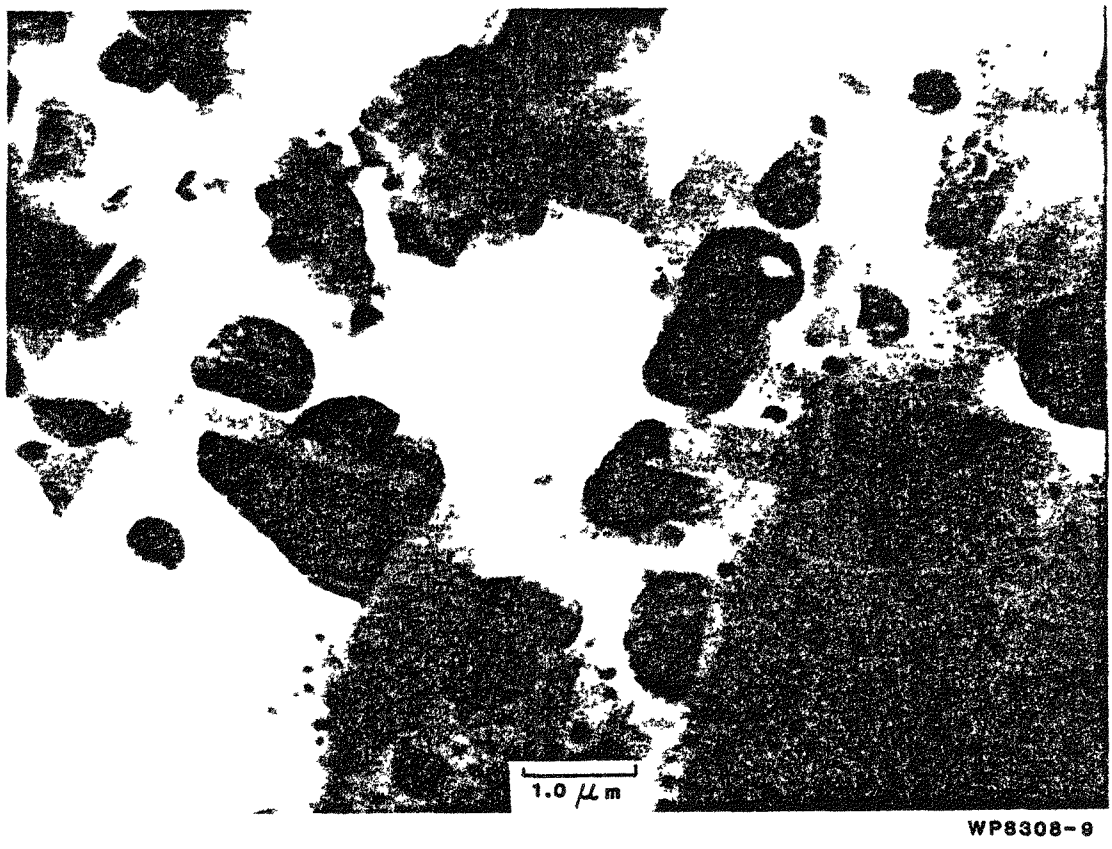

Figure 8. STEM photograph of RCE-1 glass. Lath-shaped crystals are plagioclase. Dark subrounded blebs contain pyroxene, magnetite, and apatite microcrystals.

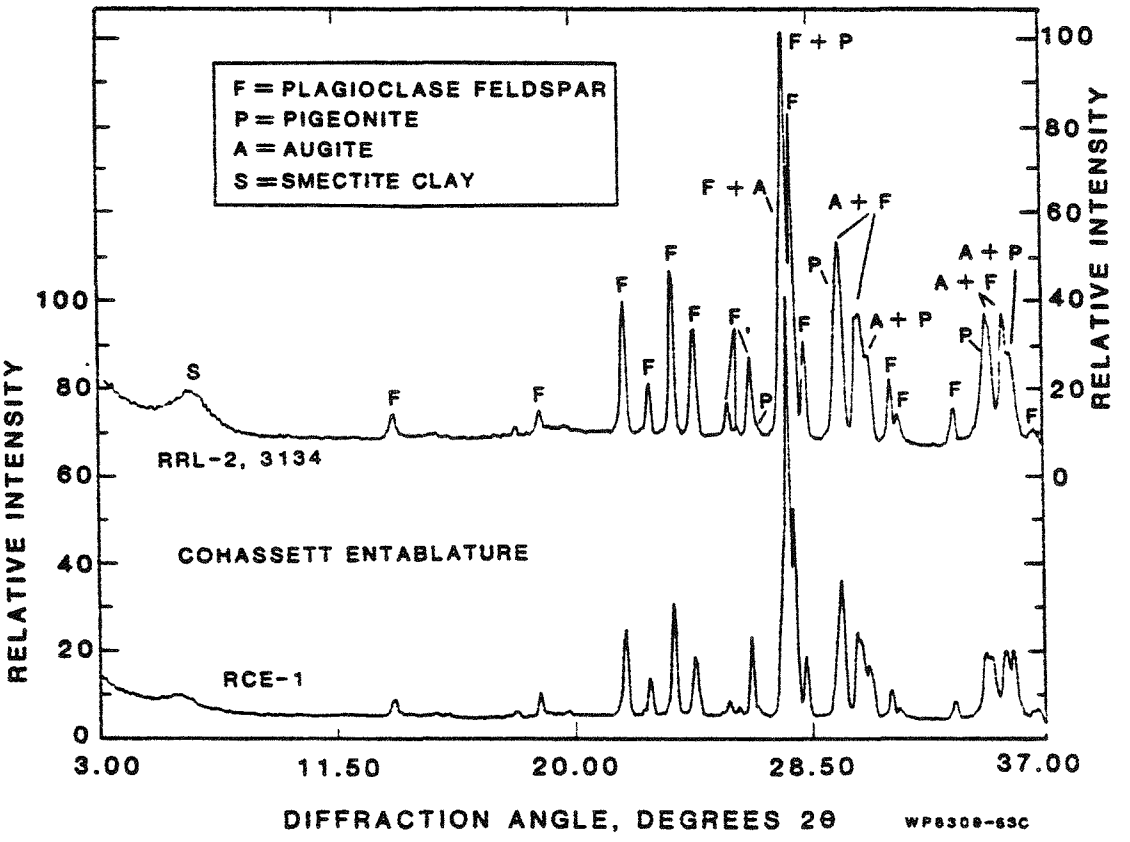

Figure 9. X-ray diffractograms of Cohassett entablature basalt from a core sample (RRL-2, 3134) and a surface sample (RCE-1).

diffraction pattern provides good matches with two PDF patterns (18-1202: $An_{67.2}$, $Ab_{31.5}$, $Or_{1.35}$; 9-465: $An_{64.5}$, $Ab_{37.2}$, $Or_{2.8}$), listed as intermediate and low sodian anorthite, respectively. Small differences in the peak positions relative to the reference diffractograms are consistent with the composition of the plagioclase (more sodic than the reference materials) as determined by electron microprobe. Most of the remainder of the basalt diffractogram is accounted for by clinopyroxenes, predominately augite (PDF 24-203), along with a smaller amount of pigeonite (PDF 13-421). The alteration products observed in the petrographic studies appear in the X-ray diffractograms as the third most abundant phase. The single peak, although weak, suggests that the phase is a smectite clay. The titaniferous magnetite observed optically and by SEM imaging could not be identified by XRD, due to the small quantity present and overlaps of the major magnetite diffraction peaks with those of more abundant phases. Similarly, the trace quantity of apatite (Table 9) was not observed by XRD. The microcrystalline plagioclase and pyroxenes in the mesostasis contribute to the diffractograms produced by their larger counterparts in the basalt. Indications of the glassy phase, which comprises at least half of the mesostasis and thus around 15 modal % of the basalt (see Table 9) are not present in the diffractogram.

As can be seen in Figure 9, the differences between surface and core samples of the Cohassett entablature basalt are relatively minor. Also, the Umtanum and Cohassett entablature basalts are quite similar, as shown in Figure 10. The primary difference occurs in the pyroxenes, relecting the much smaller quantity of pigeonite present in the Cohassett entablature relative to the Umtanum entablature (Long and Strope, 1983, p. 2). The plagioclase feldspar in the Umtanum entablature samples, based on a comparison of diffraction line positions, is slightly more albitic. This observation is consistent with the composition data for the two basalts.

The evidence for mesostasis glass seen in the diffraction pattern of Umtanum entablature basalt is not seen in the diffractogram of the Cohassett entablature, further evidence of the lesser quantity of mesostasis glass in the Cohassett flow. No smectite was seen in any of the Umtanum patterns, although evidence of a different clay phase was occasionally present.

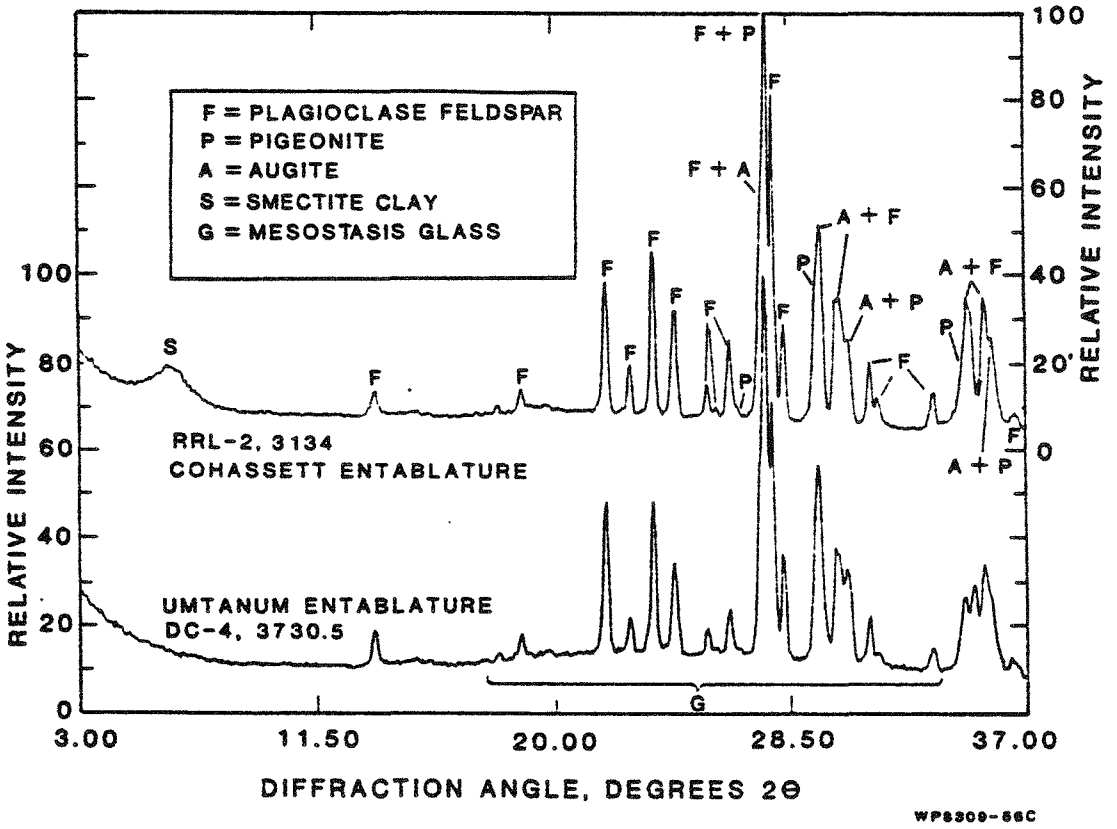

Figure 10. Comparison of X-ray diffractograms from core samples of the Cohassett and Umtanum entablature basalts. Minor differences in the primary mineral compositions are visible. No secondary clay is evident in the diffractogram of the Umtanum sample, and evidence of mesostasis glass is absent from the Cohassett pattern.

Some minor compositional variations are observed by XRD among different samples of the Cohassett entablature. The plagioclase composition varies slightly from sample to sample, as do the relative quantities of augite and pigeonite. These variations produce slight differences in the positions and intensities of the major diffraction peaks of each phase, as shown in a comparison of samples from RCE-1, RCE-2, and RCE-3 in Figure 11. Differences in clay content among the samples are also evident in the diffractograms. Preliminary analysis of RCE-4 indicates that this material has the highest clay content of the four reference Cohassett entablature samples.

X-ray Fluorescence

The bulk chemical compositions of Cohasset surfaces and core samples, as determined by XRF, are presented in Table 12. The bulk compositions of entablature and colonnade basalts are essentially identical. In addition, the average surface sample closely resembles those from depth, indicating that weathering has had minimal effect on the bulk composition of Cohassett basalt.

Summary

The Cohassett entablature, both at the reference surface location and at depth, is generally similar to the Umtanum entablature. Differences in crystal size, degree of alteration, and bulk chemical composition are considered minor. The reference Cohassett entablature material collected at the surface closely resembles Cohassett entablature basalt from the proposed repository depth, and should be an adequate substitute in geochemical tests.

Reference Cohassett Colonnade Basalt

Analysis of reference Cohassett colonnade (RCC) samples employed the suite of techniques listed above. As of this report, three sampling trips had produced reference material designated RCC-1, RCC-2, and RCC-3. In addition, previous sampling of the same horizon in the near vicinity of the reference site yielded sample C 9017 (Myers et al., 1979, Plate III-3b).

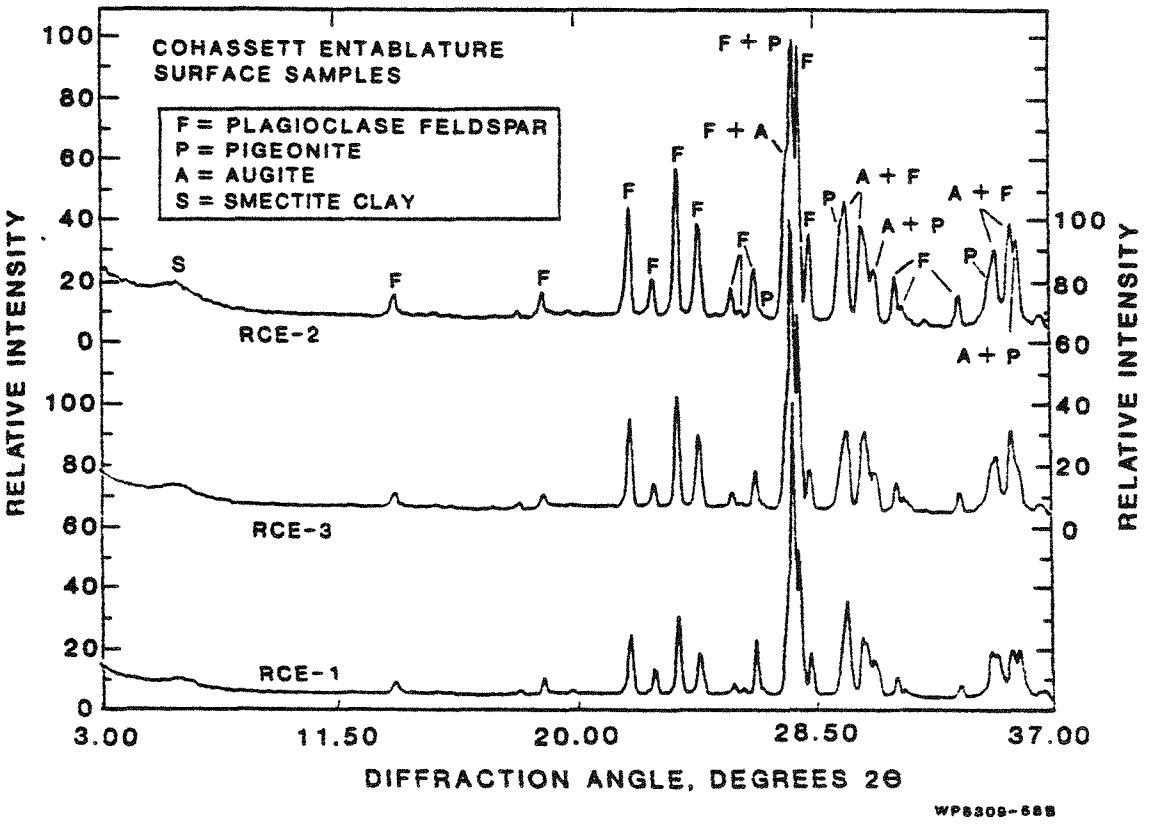

Figure 11. Comparison of X-ray diffractograms from three surface samples of reference Cohassett entablature basalt.

Table 12. Normalized Bulk Analysis by XRF of Cohassett Basalt from Surface Exposures and Core (wt%).

	Surface entablature plus colonnade[a]	Core entablature[b]	Core colonnade[c]
SiO_2	53.27	52.95	53.08
TiO_2	1.80	1.69	1.79
Al_2O_3	14.93	15.08	15.12
Fe_2O_3[d]	2.00	2.00	2.00
FeO	10.08	10.04	9.91
MnO	0.21	0.20	0.22
MgO	4.92	5.27	5.12
CaO	8.90	9.03	8.93
Na_2O	2.46	2.55	2.47
K_2O	1.13	0.94	1.10
P_2O_5	0.30	0.25	0.27
Total	100.00	100.00	100.01

[a]Myers et al., 1979, Plate III-3b.

[b]DC-2, 2556.

[c]DC-4, 3050.9.

[d]Fe_2O_3 arbitrarily set equal to 2.00.

Petrographic and Microprobe Analysis

The RCC basalt differs significantly from the entablature samples described above. While the major phases, i.e., plagioclase, pyroxene, titaniferous magnetite and mesostasis are present (Table 13), their abundances are somewhat different. In general, colonnade basalt contains a higher abundance of crystalline phases and, consequently, a lower abundance of mesostasis than entablature basalt (compare Tables 9 and 13).

The sizes and morphologies of the minor phases in colonnade and entablature samples are also different, as a comparison of Figures 12 and 7 indicates. Titaniferous magnetite crystals in colonnade samples are large and somewhat blocky. In addition, hollow needle-shaped crystals of fluorapatite with glass-filled interiors and hexagonal cross-sections (Figure 13) constitute approximately 1 modal % of many Cohassett colonnade samples. The colonnade mesostasis contains very few of the blebs which characterize the entablature mesostasis. Like the entablature basalt, the Cohassett colonnade samples, both at the surface and at depth, contain several percent alteration products, chiefly clay.

The average chemical compositions of plagioclase, pigeonite, and augite crystals in the RCC horizon are listed in Table 14. The plagioclase composition matches that of the Cohassett entablature plagioclase (see Table 10) within one standard deviation. The colonnade augite composition matches that for augite in the Cohassett entablature (Table 10 and Long and Strope, 1983, Table 1). However, the colonnade pigeonite (see Tables 14 and 10) is considerably more Fe-rich than the entablature pigeonite. Long and Strope (1983, p. 2) also noted that, in the Cohassett flow, the pigeonite/augite ratio is much larger in the colonnade than in the entablature.

The chemical composition of Cohassett colonnade glass, averaged from 58 microprobe point analyses, is listed in Table 15. Scanning electron microscopy indicates that this is actually a two-phase glass, containing one phase with a chemical composition resembling sodium-potassium feldspar and a second phase containing almost pure silica (Figure 14). The STEM electron diffraction patterns indicate a low but identifiable degree of crystallinity,

Table 13. Point Count Data* (Modal %) for the Reference Cohassett Colonnade Horizon (Sample C 9017).

	C 9017
Plagioclase	43.2
Pyroxene	24.7
Mesostasis	22.0
Titaniferous Magnetite	3.42
Apatite	0.92
Alteration Products	5.82
Total	100.1

Points Counted = 4,000

* Analyses by K. R. Fairchild

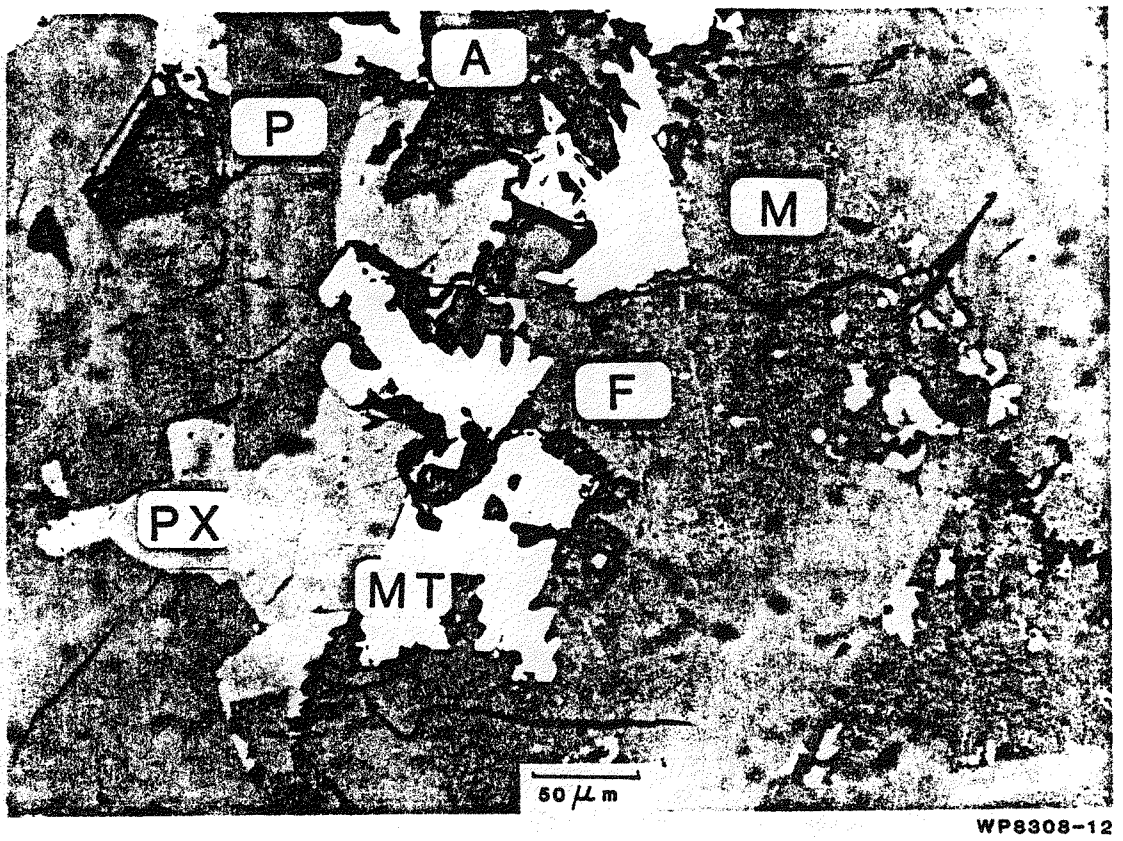

Figure 12. Reflected light photomicrograph of RCC-1 basalt. Plagioclase (P), pyroxene (PX), mesostasis (M), magnetite (MT), fluorapatite (F), alteration (A).

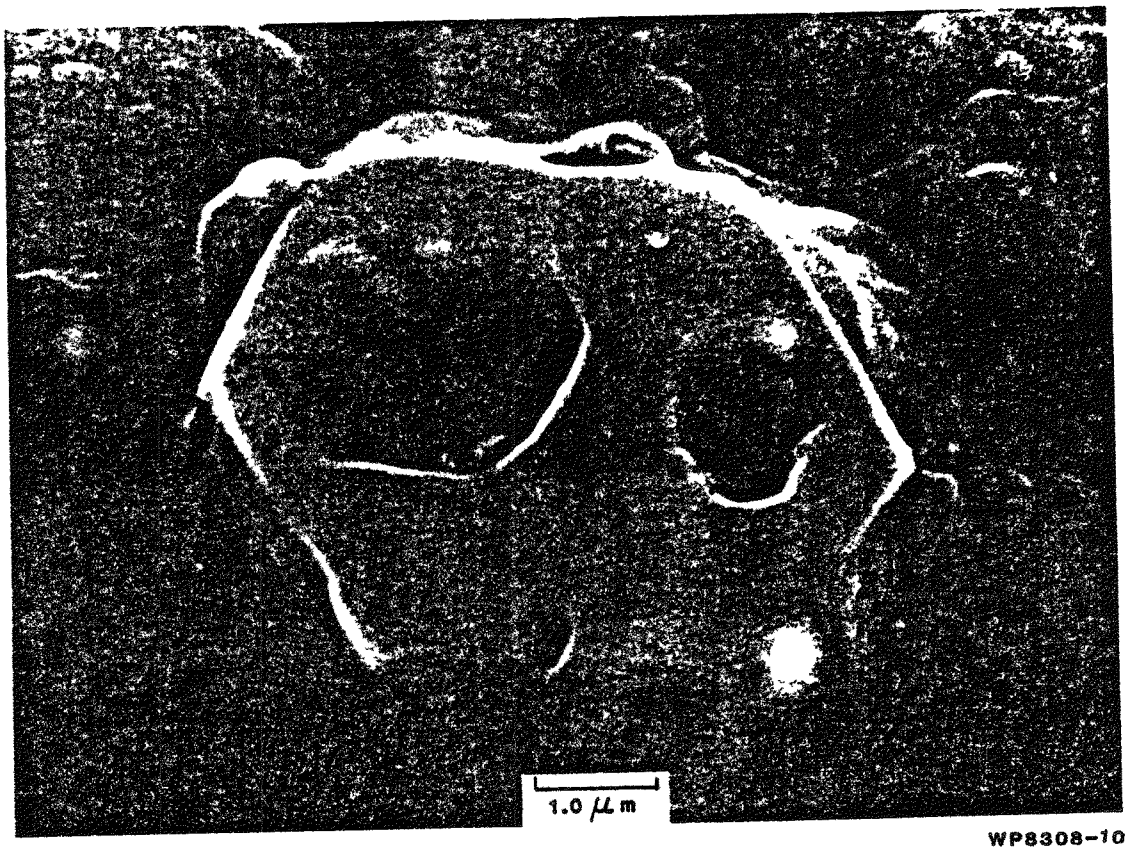

Figure 13. SEM photograph of a fluorapatite crystal, viewed end-on, in RCC-1 basalt. The crystal is hollow and filled with glass.

Table 14. Compositions of Major Silicate Minerals (wt%) from the Reference Cohassett Colonnade Horizon (Sample C 9017)

	Plagioclase		Pigeonite		Augite	
	$\bar{x}$	σ	$\bar{x}$	σ	$\bar{x}$	σ
SiO_2	54.7	1.7	49.8	0.7	52.6	0.4
TiO_2	0.1	0.1	0.6	0.1	0.6	0.1
Al_2O_3	27.7	1.7	0.6	0.1	1.7	0.2
FeO*	0.8	0.2	32.4	1.5	10.2	1.1
MnO	---	---	0.8	0.1	0.4	0.1
MgO	0.1	0.1	10.7	1.2	16.8	0.5
CaO	10.7	1.7	5.4	0.8	17.3	0.5
Na_2O	5.0	0.6	0.1	0.0	0.2	0.1
K_2O	0.4	0.3	---	---	---	---
P_2O_5	---	---	---	---	---	---
Total	99.5		100.4		99.8	
mol %	Albite 45 Orthoclase 2 Anorthite 53		Enstatite 33 Wollastonite 12 Ferrosilite 55		Enstatite 48 Wollastonite 36 Ferrosilite 16	

Points Analyzed by microprobe = 58

$\bar{x}$ Mean

σ Standard Deviation

* All Fe reported as FeO.

Table 15. Composition of Mesostasis Glass (wt%) from the Reference Cohassett Colonnade Horizon (Sample C 9017).

	$\bar{x}$	σ
SiO_2	72.5	2.0
TiO_2	0.6	0.2
Al_2O_3	12.1	1.8
FeO*	1.8	0.6
MnO	---	---
MgO	---	---
CaO	0.7	0.5
Na_2O	2.7	1.0
K_2O	5.7	0.8
P_2O_5	---	---
Total	96.1	

Points analyzed by microprobe = 58

$\bar{x}$ = Mean

σ = Standard Deviation

*All Fe reported as FeO

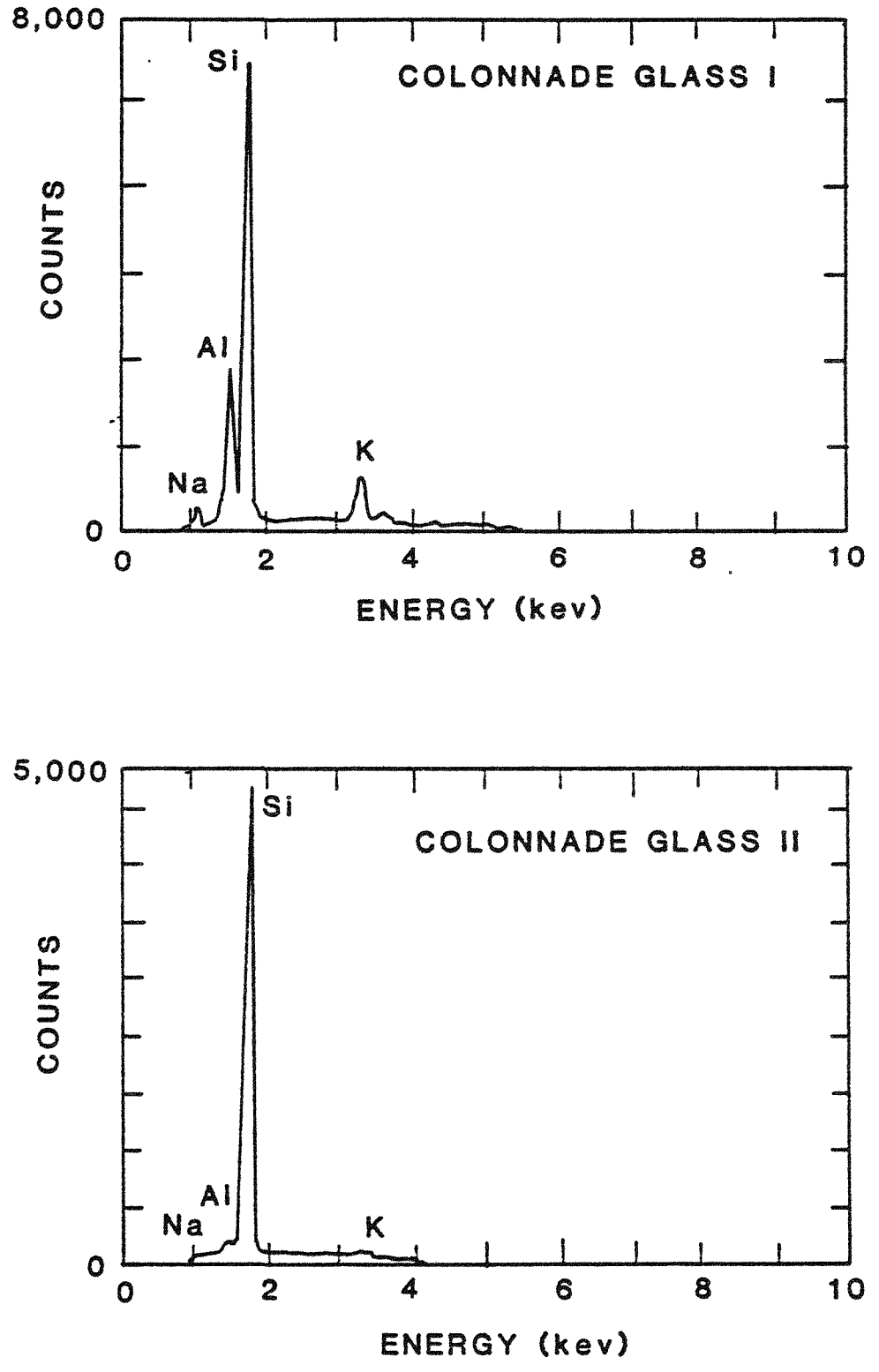

Figure 14. EDS spectra of two chemically distinct phases in Cohassett colonnade glass (Sample RRL-2, 3173).

tending toward feldspar and quartz respectively, in these two optically amorphous glass phases.

X-ray Diffraction

Differences between Cohassett colonnade basalt and material from the entablature of the flow are apparent in diffractograms of the samples. Diffractograms of Cohassett colonnade (RRL-2, 3173) and entablature RRL-2, 3134) basalts are compared in Figure 15. As in the entablature, the primary constituent of the colonnade basalt is plagioclase feldspar. The diffractogram produced by this phase is nearly identical to that of the feldspar in the entablature, providing evidence of their very similar chemistries. The bulk of the remaining diffraction lines are accounted for by the clinopyroxenes augite and pigeonite. The overall line shapes differ from those seen in the entablature diffractogram, and the augite lines appear to have shifted slightly towards smaller interplanar spacings, allowing better resolution of the pigeonite peaks. The augite peak shifts indicate a change in its chemistry. Both phases match the same reference diffraction patterns as do their counterparts in the entablature, although the augite pattern provides a better match in the colonnade than it does in the entablature pattern. The clay peak present in the diffractogram of the entablature basalt is also present in the diffractogram of the colonnade basalt. The weaker diffraction peak indicates a smaller quantity of clay is present in the colonnade than in the entablature. No clear evidence for titaniferous magnetite is observed in the diffractograms. The amorphous hump typically produced by glassy phases is absent, indicating that mesostasis glass is not present in quantities detectable by X-ray diffraction.

The colonnade samples collected on the surface differ only slightly from the core sample, as is shown in the comparison of RCC-2 basalt and core specimen diffractograms in Figure 16. Some compositional variations do apparently occur among surface samples RCC-1, RCC-2, and RCC-3, (Figure 17). The clay contents differ among the samples, and the plagioclase in RCC-1 appears to be more albitic, as evidenced by the changes in plagioclase peak positions and intensities.

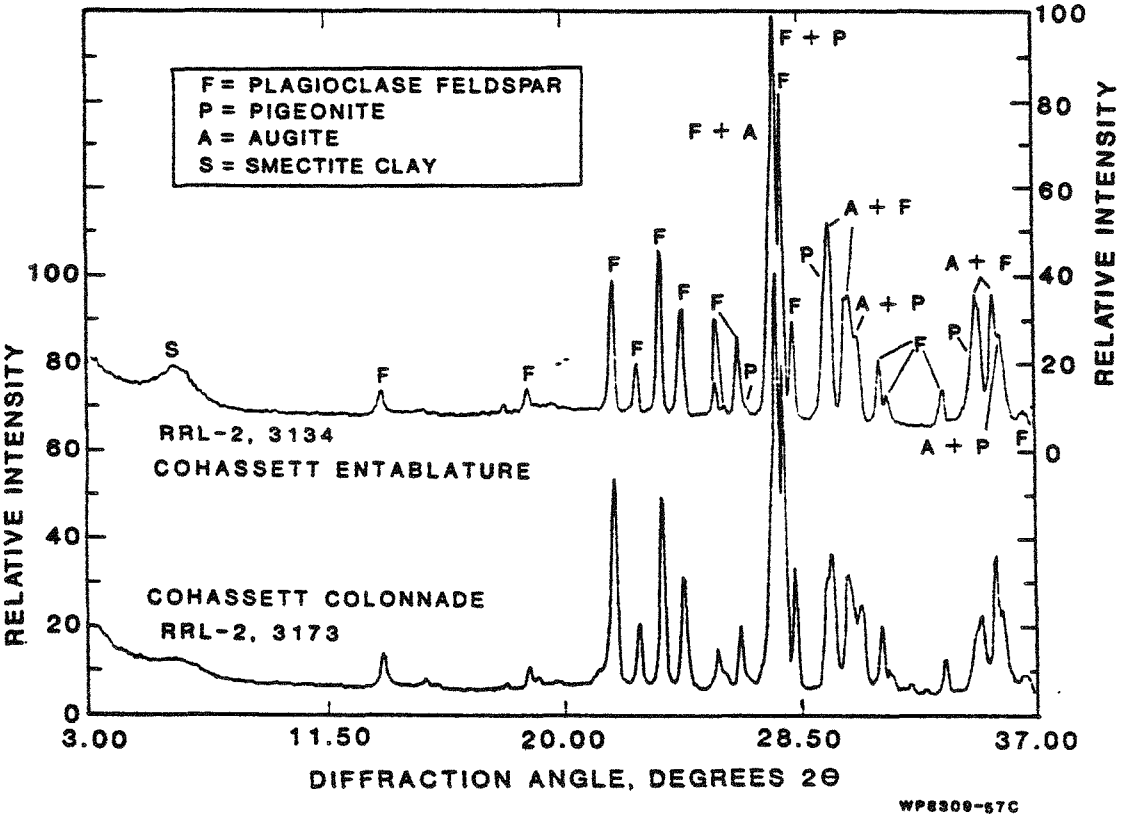

Figure 15. X-ray diffractograms of Cohassett entablature and colonnade samples from core hole RRL-2. Note the differences in the augite peaks, as well as in the intensities of the smectite clay peaks.

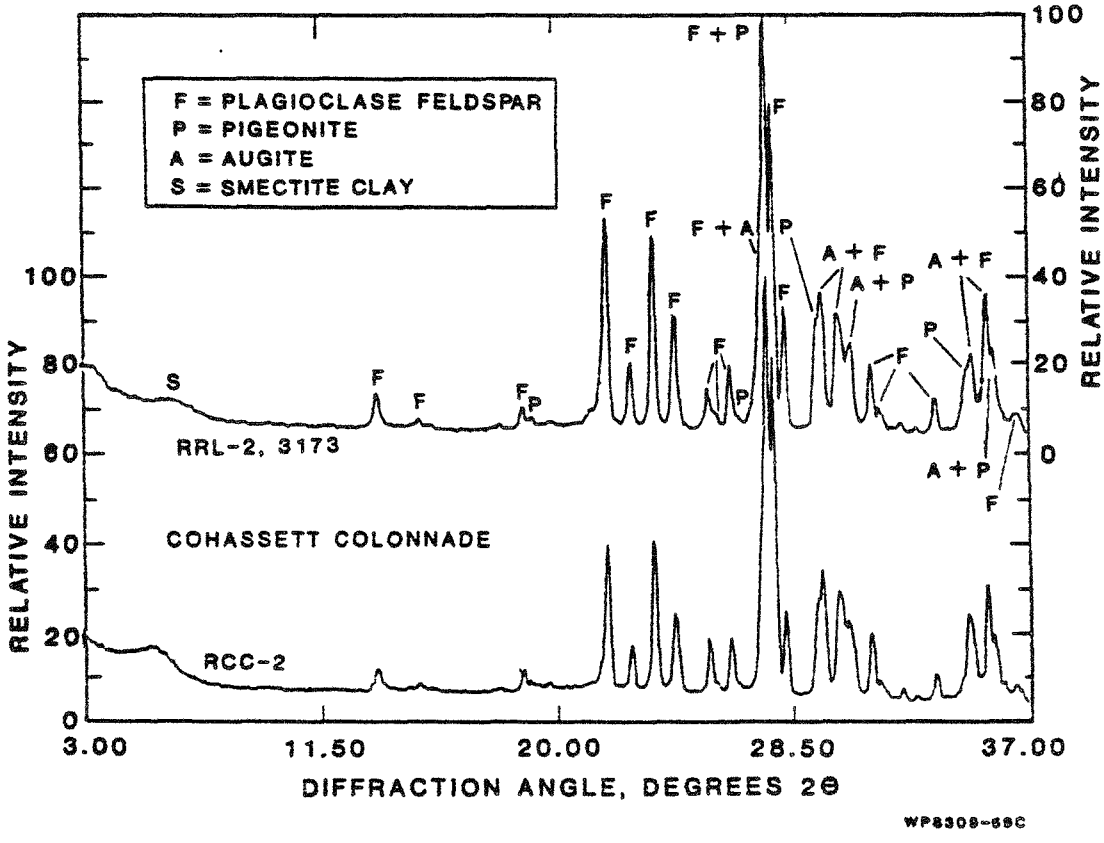

Figure 16. Comparison of X-ray diffractograms of Cohassett colonnade basalt from a core sample (RRL-2, 3173) and a surface sample (RCC-2). Only very minor differences are evident.

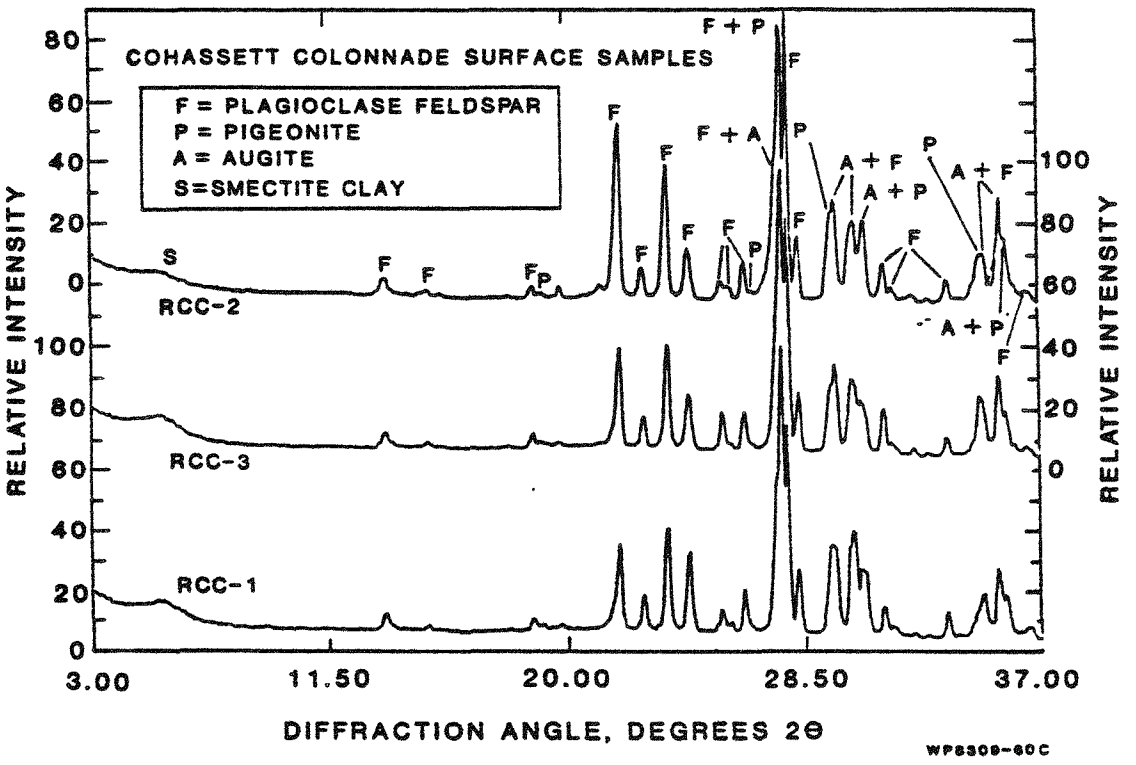

Figure 17. Comparison of X-ray diffractograms from three surface samples of reference Cohassett colonnade basalt. Differences among these patterns are indicative of the small compositional variations observed in this material by other methods.

X-ray Fluorescence

The bulk chemical composition of Cohassett colonnade basalt, as determined by XRF, is given in Table 12. No significant differences exist between the bulk compositions of colonnade and entablature samples, or between samples collected at the surface and from deep drill cores.

Summary

The Cohassett colonnade basalt, both at the reference surface site and at depth, resembles the Cohassett entablature in bulk chemical composition and major mineralogy. The late-stage cooling of the colonnade lava was apparently slower than that of the entablature lava (Wood and Long, 1984), as indicated by the larger magnetite and apatite crystals and the more "evolved" (higher silicon) glass composition in the colonnade samples. The colonnade glass is a two-phase mixture which displays incipient crystallinity. Surface samples from the reference horizon are very similar to Cohassett colonnade core samples, and should prove to be adequate substitutes in geochemical tests.

ACKNOWLEDGEMENTS

The authors would like to thank K. R. Fairchild, S. B. Kunkler, and J. R. Smith for assistance in the experimental phase of this investigation, D. G. Horton for a careful peer review, and K. L. Tomac for her cheerful secretarial help. Portions of this document are based on Sections 4.1.1 and 4.2.2 of Palmer et al., (1982), and are included here for completeness.

REFERENCES

Allen, C. C., and M. B. Strope (1983). Microcharacterization of Basalt--Considerations for a Nuclear Waste Repository, RHO-BW-SA-294 P, Rockwell Hanford Operations, Richland, Washington.

Long, P. E., and M. B. Strope (1983). Composition of Augite and Pigeonite in Basalt Flows that are Candidates for a Nuclear Waste Repository, RHO-BW-SA-295 P, Rockwell Hanford Operations, Richland, Washington.

Myers, C. W., S. M. Price, J. A. Caggiano, M. P. Cochran, W. J. Czimer, N. J. Davidson, R. C. Edwards, K. R. Fecht, G. E. Holmes, M. G. Jones, J. R. Kunk, R. D. Landon, R. K. Ledgerwood, J. T. Lillie, P. E. Long, T. H. Mitchell, E. H. Price, S. P. Reidel, and A. M. Tallman (1979). Geologic Studies of the Columbia Plateau: A Status Report, RHO-BWI-ST-4, Rockwell Hanford Operations, Richland, Washington.

Noonan, A. F., K. Fredriksson, and J. Nelen (1981). "Phase Chemistry of the Umtanum Basalt, A Reference Repository Host in the Columbia Plateau," pp. 51-58 in Scientific Basis for Nuclear Waste Management, Vol. 3, J. G. Moore, ed., Plenum Press, New York.

Palmer, R. A., G. D. Aden, R. G. Johnston, T. E. Jones, D. L. Lane., and A. F. Noonan, (1982). Characterization of Reference Materials for the Barrier Materials Test Program, RHO-BW-ST-27P, Rockwell Hanford Operations, Richland Washington.

PDF (Mineral Powder Diffraction File) (1983). International Centre for Diffraction Data, Swarthmore, PA.

Salter, P. F., L. L. Ames, and J. E. McGarrah (1981). The Sorption Behavior of Selected Radionuclides on Columbia River Basalts, RHO-BWI-LD-48, Rockwell Hanford Operations, Richland, Washington.

Wood, B. J., and P. E. Long (1984). Structures, Textures, and Cooling Histories of Columbia River Basalt Flows, RHO-BWI-SA-148 A, Rockwell Hanford Operations, Richland, Washington.